Bulletin of the Institute of Mathematics
Academia Sinica (New Series)
Vol. **11** (2016), No. 1, pp. 179-216

A MODEL REDUCTION METHOD FOR ELLIPTIC PDES WITH RANDOM INPUT USING THE HETEROGENEOUS STOCHASTIC FEM FRAMEWORK

THOMAS Y. HOU[a], PENGFEI LIU[b] AND ZHIWEN ZHANG[c]

Applied and Computational Mathematics, California Institute of Technology, Pasadena, CA 91125, USA.
[a]E-mail: hou@cms.caltech.edu
[b]E-mail: plliu@caltech.edu
[c]E-mail: zhangzw@caltech.edu

Abstract

We introduce a model reduction method for elliptic PDEs with random input, which follows the heterogeneous stochastic finite element method framework and exploits the compactness of the solution operator in the stochastic direction on local regions of the spatial domain. This method consists of two stages and suits the multi-query setting. In the offline stage, we adaptively construct local stochastic basis functions that can capture the stochastic structure of the solution space in local regions of the domain. This is achieved through local Hilbert-Karhunen-Loève expansions of sampled stochastic solutions with randomly chosen forcing functions. In the online stage, for given forcing functions, we discretize the equation using the heterogeneous coupling of spatial basis with the constructed local stochastic basis, and obtain the numerical solutions through Galerkin projection. Convergence of the online numerical solutions is proved based on the thresholding in the offline stage. Numerical results are presented to demonstrate the effectiveness of this model reduction method.

1. Introduction

Analysis of complex systems requires not only a fine understanding of the underlying physics, but also recognition of the intrinsic uncertainties and their influences on the quantities of interest (QoIs). Uncertainty Quantification (UQ) is an emerging discipline that aims at addressing the latter issue

Received April 20, 2015 and in revised form September 16, 2015.
AMS Subject Classification: 65N30.
Key words and phrases: Model reduction, local stochastic basis, Hilbert-Karhunen-Loève expansion.

and has attracted growing interest recently. In this work we consider UQ of the following second order linear elliptic equation with random input data, which can be used to model diffusion processes,

$$\begin{cases} -\mathrm{div}\,(a(x,\omega)\nabla u(x,\omega)) = f(x), \quad x \in D, \quad \omega \in \Omega, \\ u(x,\omega)|_{\partial D} = 0. \end{cases} \tag{1.1}$$

Here D is a bounded convex polygon domain in R^d, and $(\Omega, \mathcal{F}, P)$ is a probability space. We simply assume that $\Omega \subset R^m$, and the dimension of the stochastic input ω is m. We also assume that $f(x) \in L^2(D)$, and $a(x,\omega)$ is bounded and uniformly elliptic, i.e., there exist $\lambda_{\min}$ and $\lambda_{\max}$ such that

$$P(\omega \in \Omega : \ a(x,\omega) \in [\lambda_{\min}, \ \lambda_{\max}], \quad \forall x \in D) = 1. \tag{1.2}$$

The existence of solution to (1.1) is a consequence of the Lax-Milgram theorem, and we have

$$\|u(x,\omega)\|_{L^2(H_0^1(D),\Omega)} \le C\|f(x)\|_{H^{-1}(D)}, \tag{1.3}$$

where $L^2(H_0^1(D),\Omega)$ is the Hilbert space of functions $u(x,\omega)$ that satisfy

$$\|u(x,\omega)\|_{L^2(H_0^1(D),\Omega)} = \left(\int_\Omega \|u(x,\omega)\|^2_{H_0^1(D)} \mathrm{d}P\right)^{1/2} < +\infty. \tag{1.4}$$

There exist a vast literature on numerically solving stochastic partial differential equations (SPDE), and we list a few of those related to our present work below. Perturbation methods [30, 1, 28] start with expanding the stochastic solution via Taylor expansion and result in a system of deterministic equations by truncating after certain order. One limitation of perturbation methods is that the magnitude of the input and output uncertainty must be small compared with their respective means. Monte Carlo type methods [10, 36] sample the stochastic equation according to the underlying probability distribution, and compute the statistics of the solutions based on these samples. The main issue for Monte Carlo type methods is that the root-mean-square error decays very slowly as $O(M^{-1/2})$, where M is the number of samples. The polynomial chaos methods [2, 48, 37, 43, 3, 32, 49, 20] exploit the smooth dependence of the solution on the random variables, and

discretize the equation using orthogonal polynomials in the stochastic direction to achieve spectral accuracy. Polynomial chaos methods suffer from the *curse of dimensionality* since the degree of freedom grows exponentially fast with the stochastic dimension.

Efficient computation of SPDE with high dimensional stochastic input remains as an outstanding challenge. For these challenging problems there exist some methods [16, 23, 19, 5, 29, 18, 42, 9, 8, 7], that exploit the sparsity of the expansion of $u(x, \omega)$ with respect to the polynomial chaos to reduce the computational cost. Several types of model reduction methods have been proposed for these challenging problems with high stochastic dimension, including the dynamic orthogonal formulation [13, 14, 35, 41, 15] for time-dependent problems, the principal generalized decomposition method [45, 38, 22], low-rank decomposition of the stochastic solutions [12, 17], and the reduced basis method [40, 4, 39].

These high stochastic dimension problems become even more challenging in the multi-query setting where the equations need to be solved for multiple times with different forcing functions $f(x) \in L^2(D)$ or boundary conditions. For the multi-query problems, the model reduction methods mentioned above may not be efficient since one needs to construct the optimal reduced basis functions for each query. Another approach of model reduction [12, 26] is to construct a set of basis functions that can approximate the whole solution space for a family of boundary conditions and forcing functions. The identification of such a set of basis functions may be expensive, but once they are constructed, effective reduced model can be built and the computation cost for each query can be significantly reduced. In [12], the authors construct problem-dependent stochastic basis functions through Karhunen-Loève expansion of sampled stochastic solutions, and use these data-driven stochastic basis functions, instead of orthogonal polynomials to discretize the equation. In [26], the authors propose a heterogeneous stochastic finite element method (HSFEM) framework, which uses the heterogeneous coupling of spatial basis functions with local stochastic basis functions to approximate the solution space. This framework allows us to exploit the compactness of the solutions space in the stochastic direction on local regions of the spatial domain. We will follow the HSFEM framework in this paper and propose a method suited for the multi-query setting.

The staring point of our method is the compactness of the solution operator in the stochastic direction, which is a direct consequence of the fact that we have assumed the forcing function $f(x)$ to be in $L^2(D)$, not just $H^{-1}(D)$. Like many other model reduction techniques, our method consists of offline and online stages. In the offline stage, we first cover the physical domain D using overlapping sub-domains $D_i, i = 1, \dots N$, and build the corresponding partition of unity functions $\psi_i(x)$. We employ the methodology of randomized range finding algorithms and randomly choose several $L^2(D)$ forcing functions $f_1(x), \dots f_K(x)$. Then we solve the equation (1.1) using existing SPDE solver to get the corresponding solutions $u_i(x, \omega)$, $i = 1, 2 \dots K$, and restrict these sampled stochastic solutions to each sub-domain D_i. The local stochastic basis functions on D_i are adaptively extracted from the sampled solutions through the local Hilbert-Karhunen-Loève expansions, based on some *a posteriori* error estimates, and can accurately capture the local stochastic structure of the solution space. Then we construct the tensor product of local stochastic basis functions with local spatial basis functions to approximate the local solution space on each D_i. These local approximation spaces are then combined together using the partition of unity functions to get the final offline trial space V_h. In the online stage, we obtain the numerical solution $u_h(x, \omega)$ from the constructed offline trial space V_h through the Galerkin projection. Since the total degree of freedom in our method is significantly less than that of the polynomial chaos methods, we can achieve considerable computational savings in the online stage.

Compared with the previous work [26], our present work has the following features: 1) the use of the Hilbert-Karhunen-Loève expansion, the *a posterior* error estimates, and the partition of the unity formulation allow us to prove the convergence of the online numerical solution (with high probability); 2) the constructed local stochastic basis functions are the same for spatial basis functions supported on the same local region, thus we can achieve significant savings on the storage of the local stochastic basis.

This rest of this paper is organized as follows. In section 2, we show the compactness of the solution operator to equation (1.1) and review the Heterogeneous Stochastic FEM framework. In section 3, we detail the construction of the local stochastic basis functions through Hilbert-Karhunen-Loève expansions of sampled solutions in the offline stage, and the Galerkin projection procedure in the online stage. We also prove the convergence of

the online numerical solution. In section 4, we address several issues regarding the practical implementation of our method. In section 5, we present numerical results to demonstrate the efficiency of our method. Concluding remarks are made in section 6.

2. Review of the Heterogeneous Stochastic FEM Framework

2.1. Compactness of the solution operator

Using the Lax-Milgram theorem, we can obtain that for $f(x) \in H^{-1}(D)$, the solution to equation (1.1) has the following upper and lower bounds,

$$\begin{aligned} \|u(x,\omega)\|_{L^2(H_0^1(D),\Omega)} &\leq C\|f(x)\|_{H^{-1}(D)}, \\ \|u(x,\omega)\|_{L^2(H_0^1(D),\Omega)} &\geq c\|f(x)\|_{H^{-1}(D)} \end{aligned} \tag{2.1}$$

where c and C depend only on $\lambda_{\min}$ and $\lambda_{\max}$ (1.2). We denote the solution space of (1.1) for $f(x) \in H^{-1}(D)$ as V, and according to (2.1), V is a closed subspace of $L^2(H_0^1(D),\Omega)$. We denote L^{-1} as the linear operator that maps from $f(x) \in H^{-1}(D)$ to V, then (2.1) implies that L^{-1} is a homeomorphism. We denote $I_{L^2(D)\to H^{-1}(D)}$ as the embedding operator from $L^2(D)$ to $H^{-1}(D)$, which is compact according to the Sobolev space theory [21]. Then the solution operator to equation (1.1),

$$T: \quad f(x) \in L^2(D) \to u(x,\omega) \in L^2(H_0^1(D),\Omega), \tag{2.2}$$

has the following decomposition,

$$T = L^{-1} I_{L^2(D)\to H^{-1}(D)}. \tag{2.3}$$

The compactness of T follows immediately from the compactness of $I_{L^2(D)\to H^{-1}(D)}$ and the continuity of L^{-1}. To quantify the compactness of T, we introduce the definition of Kolmogorov n-width.

Definition 2.1 (Kolmogorov n-width)**.** Denote A as a bounded set in banach space X, and let X_n be an n-dimensional subspace of X, then the Kolmogorov n-width of A is

$$d_n(A) = \inf_{X_n} \sup_{x\in A} \inf_{y\in X_n} \|x-y\|. \tag{2.4}$$

The Kolmogorov n-width of the image of unit ball under T, namely, $T(B_0(1))$, characterizes the approximability of T using low rank operators. And we introduce the following definition,

Definition 2.2 (Approximability of a compact operator)**.** For a compact linear operator T, we define $d_n(T)$ that measures the approximability of T using a rank-n operator,

$$d_n(T) = \inf_{T_n} \|T - T_n\|, \tag{2.5}$$

where T_n runs over rank-n linear operators.

One can easily verify that $d_n(T) = d_n(T(B_0(1)))$.

Due to the fact that L^{-1} is a homeomorphism, (2.1), the approximability of T is of the same order as that of $I_{L^2(D)\to H^{-1}(D)}$. To be specific, based on (2.3) and (2.1), we have

$$d_n(T) = \inf_{T_n} \|T - T_n\| = \inf_{T_n} \|L^{-1}(I_{L^2(D)\to H^{-1}(D)} - LT_n)\|, \tag{2.6}$$

$$\leq C \inf_{T_n} \|I_{L^2(D)\to H^{-1}(D)} - LT_n\| = C \inf_{I_n = LT_n} \|I_{L^2(D)\to H^{-1}(D)} - I_n\|. \tag{2.7}$$

Note that $I_n = LT_n$ runs over all rank-n operator from $L^2(D)$ to $H^{-1}(D)$, so we get $d_n(T) \leq Cd_n(I_n)$. Similarly, using the lower bound in (2.1), we get $d_n(T) \geq cd_n(I_n)$. Altogether, we obtain that

$$d_n(T) \in [cd_n(I), Cd_n(I)], \tag{2.8}$$

where c and C depend on $\lambda_{\min}$ and $\lambda_{\max}$, but *do not depend on* the dimension of ω.

The compactness of $I_{L^2(D)\to H^{-1}(D)}$ is well known, see [6, 33, 27]. The following theorem can be obtained by analyzing the eigenvalues of the Laplace operator. See [6].

Theorem 2.1 (Compactness of $I_{L^2(D)\to H^{-1}(D)}$)**.**

$$d_N(I) = \frac{1}{2\sqrt{\pi}} \left(\frac{|D|}{\Gamma(1 + d/2)N} \right)^{1/d} (1 + o(1)), \quad N \to \infty, \tag{2.9}$$

where d is the dimension of the physical domain D.

The above theorem and (2.8) imply that

$$d_N(T) = O(N^{-1/d}). \tag{2.10}$$

As a consequence, there exist $O(h^{-d})$ basis functions in $L^2(H_0^1(D), \Omega)$, such that for any $f(x) \in L^2(D)$ and the corresponding solution to (1.1) $u(x, \omega)$, we have the following approximation property

$$\inf_{v(x,\omega)\in V_h} \|u(x, \omega) - v(x, \omega)\|_{L^2(H_0^1(D),\Omega)} \leq h\|f\|_{L^2(D)}, \tag{2.11}$$

where V_h is the finite dimensional space spanned by these $O(h^{-1/d})$ basis functions.

Note that in (2.11), the number of basis functions required to obtain the $O(h)$ approximation accuracy is $O(h^{-d})$, and this is optimal and independent of the stochastic dimension. It is a direct consequence of the uniform ellipticity of the equation (1.2), and our assumption that the forcing function $f(x)$ has higher integrability, namely it lives in $L^2(D)$, not just $H^{-1}(D)$. This fact implies that the model (1.1) with high dimensional stochastic input can, *at least in principle*, be effectively reduced.

2.2. The heterogeneous stochastic FEM framework

Due to the global nature of the elliptic operator in (1.1), it is in general not easy to construct an effective set of basis functions to obtain the optimal approximation property (2.11). Besides, we hope that these basis functions have compact support so that the corresponding stiffness matrix in the Galerkin projection is sparse and easy to invert. For the above reasons, we *give up* the optimal approximation property (2.11) and seek to construct basis functions that have *compact support* and are easy to represent.

For deterministic elliptic equations, the piecewise linear basis functions are employed to approximate the solution space [44]. In the stochastic setting, we use the product of these spatial basis with some stochastic basis to approximate the solution. And this leads us to the heterogeneous stochastic finite element (HSFEM) framework proposed in [26]. The HSFEM framework employs a finite dimensional subspace of $L^2(H_0^1(D), \Omega)$ taking the fol-

lowing form to discretize equation (1.1),

$$V_h = \Big\{ \sum_{i=1}^{n} \sum_{j=0}^{k_i} c_i^j \phi_i(x) \xi_i^j(\omega) \Big\}. \tag{2.12}$$

The $\phi_i(x), i = 1, \dots n$ are a set of finite element spatial basis functions, and $\xi_i^j(\omega), j = 0, \dots k_i$ are the stochastic basis functions associated with $\phi_i(x)$. The key feature of the above finite dimensional space is that different stochastic basis functions are used to couple with different spatial basis functions. Since $\phi_i(x)$ has local support, the associated stochastic basis $\xi_i^j(\omega), j = 0, \dots k_i$ are called *local stochastic basis*. The above finite-dimensional space allows for spatially heterogeneous stochastic structure of the solution space. The numerical results obtained in [26] reveal that the solution spaces to elliptic equations with several types of random input have strong spatially heterogeneous stochastic structure, which justifies the use of the HSFEM framework for stochastic elliptic equations.

After constructing the trial space (2.12) that has good approximation property, we can obtain numerical solution $u_h(x, \omega)$ through the Galerkin projection. Namely, we seek $u_h(x, \omega) \in V_h$, such that

$$\int_\Omega \int_D \nabla u(x, \omega) a(x, \omega) \nabla v(x, \omega) \mathrm{d}x \mathrm{d}P = \int_\Omega \int_D f(x) v(x, \omega) \mathrm{d}x \mathrm{d}P, \tag{2.13}$$

for all $v(x, \omega) \in V_h$. The numerical solution obtained from above enjoys the following quasi-optimality

$$\|u(x, \omega) - u_h(x, \omega)\|_{L^2(H_0^1(D), \Omega)} \leq C \inf_{v(x,\omega) \in V_h} \|u(x, \omega) - v(x, \omega)\|_{L^2(H_0^1(D), \Omega)}. \tag{2.14}$$

The total number of basis functions in (2.12) is $K = \sum_{i=1}^{n} (k_i + 1) = n\bar{k} + n$, where $\bar{k}$ is the average of k_i. Correspondingly, the stiffness matrix formed in (2.13) is $K \times K$ and sparse. The success of the HSFEM framework relies on constructing V_h that has good approximating property and small k_i. Since $\phi_i(x)$ has local support near node point x_i, the associated stochastic basis functions $\xi_i^j(\omega), j = 0, \dots k_i$ approximate the stochastic structure of the solution near x_i. In [26], the following operator, which maps the forcing $f(x) \in L^2(D)$ to the stochastic part of the solution on a single node point

x_i, is investigated,

$$T_i : f(x) \in L^2(D) \to u(x_i, \omega) - \bar{u}(x_i, \omega) \in L^2(\Omega). \tag{2.15}$$

It is shown in [26] that T_i is a compact linear operator, and has the following singular value decomposition,

$$T_i f(x) = \sum_{j=1}^{\infty} \sigma_i^j \int_D f(x)\phi_i^j(x)\mathrm{d}x\xi_i^j(\omega), \tag{2.16}$$

where $\phi_i^j(x), \sigma_i^j, \xi_i^j(\omega), j = 1, \dots \infty$ are obtained from the Karhunen-Loève expansion of $G(x_i, y, \omega)$,

$$G(x_i, y, \omega) = \bar{G}(x_i, y) + \sum_{j=1}^{\infty} \sigma_i^j \phi_i^j(x)\xi_i^j(\omega). \tag{2.17}$$

$G(x_i, y, \omega)$ is the Green's function of (1.1), and the Karhunen-Loève expansion will be introduced in section 3.2. Since for the physical dimension $d = 2, 3$, $G(x_i, y, \omega) \in L^2(D \times \Omega)$, see [46, 24], we have $\sum_{j=1}^{\infty} (\sigma_i^j)^2 \leq C$, where C is independent of the stochastic dimension of the problem. Consequently, to obtain order ϵ accuracy in approximating T_i in the sense of (2.5), at most $O(\epsilon^{-2})$ stochastic basis functions are required [26]. This upper bound is obtained only under the assumption that equation (1.1) is uniformly elliptic, and it is independent of the stochastic dimension of the problem.

The numerical results in [26] show that the singular values of T_i decay exponentially fast, namely, T_i has a low rank structure. Thus a very small number of stochastic basis functions are enough to approximate the range of T_i very well in the sense of (2.5). This result illustrates the compactness of the solution operator in the stochastic direction in local regions of the domain, and reveals the potential advantage of the HSFEM framework for stochastic elliptic equations.

The HSFEM framework can be viewed as a generalization of the polynomial chaos methods by using *problem-dependent* and *local* stochastic basis functions instead of orthogonal polynomials. This generalization enables us to significantly reduce the total degree of freedom, and consequently the computational cost. In this paper, we follow the HSFEM framework, and

propose an effective method to construct the local stochastic basis functions through local Hilbert-Karhunen-Loève expansion to sampled solutions of (1.1). Compared with the previous method in [26], the present work allows us to rigorously control the error in the online numerical solution $u_h(x,\omega)$, and can bring in savings on the storage of the local stochastic basis. These will be detailed in the next section.

3. Construction of the Local Stochastic Basis through Local Hilbert-Karnuen-Loève Expansion

3.1. Local approximation of the solution space

To construct the local stochastic basis functions, we first cover the physical domain D using sub-domains $D_i, i = 1, \dots N$, and construct the partition of unity functions $\psi_i(x)$ [34] . Namely, they satisfy

$$D = \bigcup_{i=1}^{N} D_i,\ \text{support}(\psi_i(x)) \subset D_i,\ \psi_i(x) \geq 0,\ \sum_{i=1}^{N} \psi_i(x) = 1 \text{ for } x \in D. \tag{3.1}$$

We make additional assumptions about this partition of unity that the number of sub-domains D_j that intersects D_i is bounded, and

$$N \leq \frac{C}{H^d}, \quad \text{diam}(D_i) = O(H), \quad |\nabla \psi_i(x)| \leq \frac{C}{H}. \tag{3.2}$$

The above assumptions can be easily satisfied by using a uniform coarse mesh of size H.

Then we consider the solution space to (1.1) restricted on a sub-domain D_i, namely $u(x,\omega)|_{D_i}$. We seek to construct local stochastic basis functions $\xi_i^j(\omega)$, $j = 0, \dots k_i$ that capture the stochastic structure of the solution on D_i, and use the following tensor product space to approximate $u(x,\omega)|_{D_i}$,

$$V_{h,i} = \text{span}\{\xi_i^0(\omega), \xi_i^1(\omega), \dots \xi_i^{k_i}(\omega)\} \otimes \text{span}\{\phi_i^1(x), \phi_i^2(x), \dots \phi_i^{n_i}(x)\} \tag{3.3}$$

where $\phi_i^j(x)$ are the piecewise linear finite element basis functions on a fine mesh of size h and with support on D_i. In this work we focus on model reduction in the stochastic direction, thus assume for simplicity that the spatial variation of the solution can be captured accurately by the fine mesh

of size h. Namely, we neglect the error from the spatial discretization using finite dimensional space

$$\text{span}\{\phi_i^1(x), \phi_i^2(x), \dots \phi_i^{n_i}(x)\}. \tag{3.4}$$

We construct these $\xi_i^j(\omega)$ through the Hilbert-Karhunen-Loève expansion of sampled solutions.

3.2. The Hilbert-Karhunen-Loève expansion

For a stochastic process $u(x,\omega) \in L^2(D \times \Omega)$, it can be expanded in a Fourier type series as

$$u(x,\omega) = \bar{u}(x) + \sum_{i=1}^{\infty} \sigma_i \phi_i(x) \xi_i(\omega), \tag{3.5}$$

where $\phi_i(x)$ and $\xi_i(\omega)$ are orthonormal vectors in $L^2(D)$ and $L^2(\Omega)$ respectively. The above expansion (3.5) is called the Karhunen-Loève (KL) expansion of $u(x,\omega) \in L^2(D \times \Omega)$, [47, 11], and the $\phi_i(x)$ can be constructed as the eigenvectors of the covariance function $C(x,y) = \text{Cov}(u(x,\omega), u(y,\omega))$,

$$\int_D C(x,y)\phi_i(y)\mathrm{d}y = \sigma_i^2 \phi_i(x). \tag{3.6}$$

The random variable $\xi_i(x)$ can be computed as

$$\xi_i(\omega) = \frac{1}{\sigma_i} \int_D (u(x,\omega) - \bar{u}(x))\phi_i(x)\mathrm{d}x. \tag{3.7}$$

The truncated KL expansion is known as the best low rank approximation of a second order stochastic process in the $L^2(D \times \Omega)$ sense. However, for our problem, we want to construct stochastic basis $\xi_i^j(\omega), j = 0, \dots k_i$, such that the expanded tensor product space (3.3) approximates $u(x,\omega)|_{D_i}$ in $L^2(H^1(D_i), \Omega)$ sense, not $L^2(D \times \Omega)$ sense. This is because according to (2.14), the Galerkin projection formulation seeks the best approximation of the solution within the trial space in $L^2(H_0^1(D), \Omega)$. This consideration naturally leads us to the Hilbert-Karhunen-Loève expansion [17].

For a stochastic process $u(x,\omega) \in L^2(H^1(D),\Omega)$, we have the following Fourier type expansion,

$$u(x,\omega) = \bar{u}(x) + \sum_{i=1}^{\infty} \sigma_i \psi_i(x) \xi_i(\omega), \tag{3.8}$$

where $\psi_i(x)$ and $\xi_i(\omega)$ are orthonormal vectors in $H^1(D)$ and $L^2(\Omega)$ respectively. The difference between (3.8) and (3.5) is that the spatial basis $\psi_i(x)$ in (3.8) is orthonormal in $H^1(D)$, while the spatial basis $\phi_i(x)$ in (3.5) is orthonormal in $L^2(D)$.

To obtain the above Hilbert-Karhunen-Loève (HKL) expansion, we first choose a complete set of orthonormal basis in $H^1(D)$, and denote them as $\Psi_j(x)$, $j = 1, \ldots \infty$. For each $\omega \in \Omega$, we consider the projection of $u(x,\omega) - \bar{u}(x)$ on this basis, and denote the coefficients of the projection as $c(j,\omega)$. Namely,

$$u(x,\omega) - \bar{u}(x) = \sum_{j=1}^{\infty} c(j,\omega) \Psi_j(x). \tag{3.9}$$

One can easily see that $c(j,\omega) \in L^2(\mathcal{N} \times \Omega)$, where $\mathcal{N}$ is the set of natural numbers. We actually have $\|c(i,\omega)\|_{L^2(\mathcal{N}\times\Omega)} = \|u(x,\omega)\|_{L^2(H_0^1(D),\Omega)}$, thus we can do KL expansion to $c(j,\omega)$ and get

$$c(j,\omega) = \sum_{i=1}^{\infty} \sigma_i l_i(j) \xi_i(\omega), \tag{3.10}$$

where $l_i(j)$ and $\xi_i(\omega)$ are orthonormal vectors in $L^2(\mathcal{N})$ and $L^2(\Omega)$ respectively.

The above expansion combined with (3.9) gives us the Hilbert-Karhunen-Loève expansion of $u(x,\omega)$ (3.10), with $\xi_i(\omega)$ and σ_i given by (3.10), and $\psi_i(x)$ given by $\sum_{j=1}^{\infty} l_i(j)\Psi_j(x)$, namely,

$$u(x,\omega) = \bar{u}(x) + \sum_{i=1}^{\infty} \sigma_i \left(\sum_{j=1}^{\infty} l_i(j) \Psi_j(x) \right) \xi_i(\omega). \tag{3.11}$$

The first several stochastic basis functions in (3.8) capture the stochastic structure of $u(x,\omega)$, and span the best low dimensional space (3.3) approximating $u(x,\omega)|_{D_i}$ in $L^2(H^1(D_i),\Omega)$.

We will employ the philosophy of randomized range finding algorithms, and apply the HKL expansion to sampled solutions $u(x,\omega)|_{D_i}$ to construct the local stochastic basis.

3.3. Randomized range finding algorithm

The problem of constructing effective local stochastic basis functions is essentially a range-finding problem, which can be formulated as the following: for a matrix T, we want to find a matrix Q with orthonormal columns such that its column space captures the main action of T.

To be precise, we want the following holds,

$$\|T - QQ^T T\| \leq \epsilon. \tag{3.12}$$

Note that QQ^T in the above equation is the projection operator to the column space of Q.

The idea of the randomized range finding algorithms is the following: assuming that the operator T has low rank, namely, its singular values decay very fast, then the main action of T can be captured in the image of some random matrix Ω under T, $T\Omega$, with high probability. Therefore, one can extract the orthonormal matrix Q approximating the range of T from $T\Omega$ using the Gram-Schmidt orthogonalization. See [25, 31] for more about these randomized range finding algorithms. Once we have got some Q approximating the range of T, we can use the following Lemma 3.1 (see [25]) to verify that the condition (3.12) holds with high probability. To be specific, we choose the matrix B in Lemma 3.1 as $T - QQ^T T$, and draw r random vectors $\omega^{(i)}$. We use T to act on these $\omega^{(i)}, i = 1, \dots r$, and compute the residuals after projecting the images $T\omega^{(i)}$ to the column space of Q, namely $\|(I - QQ^T)T\omega^{(i)}\|$. If all the r number of residuals are smaller than $\frac{\epsilon}{\alpha}\sqrt{\frac{\pi}{2}}$, then the condition (3.12) holds except with probability α^{-r}.

Lemma 3.1. *Let B be a real $m \times n$ matrix. Fix a positive integer r and a real number $\alpha > 0$. Draw an independent family of standard Gaussian vectors*

$$\{\omega^{(i)} : i = 1, 2 \dots, r\}. \tag{3.13}$$

Then

$$\|B\| \leq \alpha\sqrt{\frac{2}{\pi}} \max_{i=1,\ldots,r} \|B\omega^{(i)}\| \tag{3.14}$$

except with probability α^{-r}.

The good thing about the randomized range-finding algorithms and the error estimation (3.14) is that they do not require access to each entry of the matrix T, and only require the matrix-vector multiplication. For our problem, this matrix-vector multiplication corresponds to solving (1.1) with certain $f(x)$, which we have access to using existing SPDE solvers. So we can employ the randomized range finding philosophy and the error estimation (3.14) in our problem to construct local stochastic basis and the corresponding tensor product space (3.3). These will be detailed in the next subsection.

3.4. Constructing local stochastic basis through HKL expansion

We consider approximating the range of operator $R_{D_i}T$ using (3.3) for our problem, where R_{D_i} is the restriction on D_i. For $f(x) \in L^2(D)$, $R_{D_i}Tf = u(x,\omega)|_{D_i}$, where $u(x,\omega)$ is the corresponding solution to (1.1). The following algorithm returns local stochastic basis functions on subdomains $D_i, i = 1, \ldots N$, such that the resulting tensor production spaces (3.3) can accurately approximate the range of $R_{D_i}T$.

1. **Discretizing the domain of T, $L^2(D)$.**

   To apply $R_{D_i}T$ to some random vector, we first discretize the domain of T, namely, $L^2(D)$. We select a complete set orthonormal basis functions of $L^2(D)$, and denote them as $\Phi_i(x)$, $i = 1, \ldots \infty$. In our numerical examples, the domain D is $[0,1]^d$, and the $L^2(D)$ basis functions are chosen to be the Fourier modes. We then use the first L basis functions $\Phi_i(x), i = 1, \ldots L$ to discretize $L^2(D)$. Note that $L^2(D)$ is infinite-dimensional, and cannot be approximated using only finite basis functions. But in practice, we discretize equation (1.1) in the spatial direction using a fine mesh of size h, thus we can discard the Fourier modes that cannot be resolved by the fine mesh without losing accuracy, see [26]. To be specific, we discretize $L^2(D)$ using the following basis,

   $$\otimes_{i=1}^{d}\{1, \ldots, 2\sin(2\pi l x_i), 2\cos(2\pi l x_i)\}, \tag{3.15}$$

where $l = 1/h$. Then the number of basis functions used to discretize $L^2(D)$ is $L = (2l+1)^d$.

2. **Constructing random vectors** (3.13) **for the purpose of error estimation**

   In the *a posteriori* error estimation procedure (3.14), we need to choose r random vectors $\omega^{(i)}, i = 1, \dots r$, and compute $T\omega^{(i)}$. In our construction of the local stochastic basis, we do this before we obtain the Q because we need the error estimation to adaptively add local stochastic basis.

   We choose r independent standard Gaussian vectors in R^L, $\omega_i(j), i = 1, \dots r, j = 1, \dots L$, and construct the corresponding r forcing functions using the $L^2(D)$ basis $\Phi_i(x)$ (3.15) chosen in the previous step. We get $f_i(x) = \sum_{j=1}^{L} \omega_i(j)\Psi_j(x), i = 1, \dots r$. Then we solve equation (1.1) using existing solver with these forcing functions $f_i(x)$. Details regarding our numerical discretization are given in section 4. We restrict the numerical solutions on each domain D_i, and denote these samples as $u_i^j(x, \omega)$, $i = 1, \dots N$, $j = 1, \dots r$.

   The above process corresponds to computing $T\omega^{(i)}, i = 1, \dots r$ in (3.14). After we get Q in step 4, we can apply $I - QQ^T$ to $T\omega^{(i)}$ to estimate $\|T - QQ^T T\|$ using Lemma 3.1.

3. **Initializing the local stochastic basis on each** D_i

   The initial local stochastic basis functions on all the subdomains D_i only contain $\xi_i^0(\omega) = 1$. During the construction process in the following steps, more local stochastic basis functions will be added.

4. **Drawing random vector** f **and extracting stochastic basis from the HKL expansion.**

   Randomly choose a $L^2(D)$ forcing function as in step 2, $f(x)$. We solve equation (1.1) using $f(x)$, and restrict the numerical solution $u(x, \omega)$ to each domain D_i. On each D_i, we compute the projection of $u(x, \omega)|_{D_i} - \bar{u}(x)|_{D_i}$ to the tensor product space (3.3) using the already constructed local stochastic basis functions. We denote the residual of the projection as $u_i^e(x, \omega)$, which contains the part of the solution that cannot be captured by the constructed local stochastic basis. Then we do the Hilbert-Karhunen-Loève expansion to the residue $u_i^e(x, \omega)$

following the procedure described in the previous section. And the $H^1(D_i)$ norm used in (3.9) is chosen to be:

$$\|u(x,\omega)|_{D_i}\|_{H^1(D_i)} = (\int_{D_i} (\frac{1}{H^2}u(x,\omega)^2 + |\nabla u(x,\omega)|^2)\mathrm{d}x)^{1/2}. \quad (3.16)$$

Note that we put a $1/H^2$ weight in front of the L^2 norm, the reason of which will be clear in our proof of the convergence of the online numerical solutions. We then add the stochastic basis in the HKL expansion of $u_i^e(x,\omega)$ to the set of local stochastic basis functions on D_i. Details concerning the discretization of the numerical solutions are given in section 4.

5. A posteriori error estimation

Then we use the newly obtained set of local stochastic basis functions on each D_i to form the tensor product space (3.3), and project the saved $u_i^j(x,\omega)$ onto this tensor product space. We compute the $L^2(H^1(D_i),\Omega)$ norm of the residuals. By doing so we are actually computing

$$\|(I - QQ^T)T\omega^{(i)}\|_{L^2(H^1(D_i),\Omega)}, \quad i = 1,\dots r. \quad (3.17)$$

If on D_i, for all the r sampled solutions $u_i^j(x,\omega)$, $j = 1,\dots r$, the residuals are less than

$$\alpha^{-1}\sqrt{\pi/2}\epsilon H^{d/2}, \quad (3.18)$$

then we mark that the construction of local stochastic basis functions on D_i is complete, and will not add local stochastic basis functions on D_i any more.

Otherwise we go back to step 4 and continue adding local stochastic basis functions until the constructions are complete on all D_i.

The above algorithm will stop within L steps. For each domain D_i, we denote the resulting tensor product space (3.3) as $V_{h,i}$, and the projection operator to $V_{h,i}$ as P_i. Then we have that for each D_i, with exceptional probability less than $L\alpha^{-r}$, the following holds,

$$\|R_{D_i}T - P_iR_{D_i}T\| \le \epsilon H^{d/2}, \quad (3.19)$$

where the norm is taken as the operator norm mapping from $L^2(D)$ to $L^2(H^1(D_i), \Omega)$. Namely, the resulting local tensor product space (3.3) can capture the local solution space on D_i.

We comment that the construction of local stochastic basis can be quite expensive since it involves solving (1.1) multiple times using existing SPDE solver. However, if the solution space has low stochastic dimension in local regions of the domain, which is observed to be true based on our numerical results, then we can construct the local stochastic basis by solving the SPDE (1.1) for only a few times.

Our model reduction method does not apply to problems where the equation (1.1) only needs to be solved for once, because the offline stage of our method already involves solving (1.1) for several times to construct the local stochastic basis. However, if the equation (1.1) needs to be solved for multiple times using different $L^2(D)$ forcing functions, then our method can offer considerable computational savings because once the local stochastic basis has been constructed, we can use them to build a reduced model with significantly less degree of freedom, and solve the equation efficiently in the online stage.

3.5. Coupling of local stochastic basis with the spatial basis

After we get the local stochastic basis functions and the corresponding tensor product space (3.3), we multiply them by the partition of unity functions $\psi_i(x)$ (3.1) and combine them together. We finally get the finite dimensional space approximating the solutions to (1.1), V_h,

$$V_h = \sum_{i=1}^{N} \psi_i(x) V_{h,i}. \tag{3.20}$$

It can be expanded as

$$V_h = \{\sum_{i=1}^{N} \sum_{j=1}^{n_i} \sum_{l=1}^{k_i} c_i^{j,l} \psi_i(x) \phi_i^j(x) \xi_i^l(\omega) : c_i^{j,l} \in R\}, \tag{3.21}$$

where i is the index of the partition of unity sub-domain D_i, j is the index of spatial basis functions on each D_i, and l is the index of the local stochastic basis function constructed on D_i.

With the above trial space, we then use the Galerkin projection method to get the numerical solution. Namely, we seek $u_h(x,\omega) \in V_h$, such that for all $i = 1, \dots N$, $j = 1, \dots n_i$, $l = 0, \dots k_i$,

$$\begin{aligned} &\int_\Omega \int_D \nabla u_h(x,\omega) a(x,\omega) \nabla(\psi_i(x)\phi_i^j(x)\xi_i^l(\omega)) \mathrm{d}x\mathrm{d}P \\ &= \int_\Omega \int_D f(x)\psi_i(x)\phi_i^j(x)\xi_i^l(\omega)\mathrm{d}x\mathrm{d}P. \end{aligned} \tag{3.22}$$

Recall that the *a posteriori* error estimation in the offline stage guarantees that, with high probability, the tensor product space (3.3) on each subdomain D_i can accurately approximate the solutions restricted on D_i. Using this local approximation property (3.19), we have the following convergence result.

Theorem 3.1. *Consider solving* (1.1) *using the trial space* (3.21)*, and the Galerkin projection* (3.30)*. Then with high probability, we have*

$$\|u(x,\omega) - u_h(x,\omega)\|_{L^2(H_0^1(D),\Omega)} \leq C\epsilon \|f\|_{L^2(D)}. \tag{3.23}$$

Recall that we have assumed the physical mesh of size h can resolve the spatial variation of the solution space, and neglect the numerical error originating from the space discretization. Namely, we focus on the error coming from the model reduction in the stochastic direction.

Proof. Based on the local approximation property (3.19), we know that with high probability, there exist $c_i^{j,l}$, $j = 1, \dots n_i$, $l = 0, \dots k_i$, such that

$$\|u(x,\omega) - \sum_{j=1}^{n_i}\sum_{l=0}^{k_i} c_i^{j,l}\phi_j(x)\xi_i^l(\omega)\|_{L^2(H^1(D_i),\Omega)} \leq \epsilon H^{d/2}\|f(x)\|_{L^2(D)}, \tag{3.24}$$

where we have neglected the discretization error in the spatial direction, and the $H^1(D_i)$ norm is the weighted norm defined in (3.16). We denote $\sum_{j=1}^{n_i}\sum_{l=0}^{k_i} c_i^{j,l}\phi_j(x)\xi_i^l(\omega)$ as $u_i^h(x)$, then according to (3.21), we have $\psi_i(x)u_i^h(x) \in V_h$. Since $\sum_{i=1}^N \psi_i(x) = 1$, we have

$$u(x,\omega) - \sum_{i=1}^N \psi_i(x)u_i^h(x,\omega) = \sum_{i=1}^N \psi_i(x)(u(x,\omega) - u_i^h(x,\omega)). \tag{3.25}$$

Then we have

$$\nabla(u(x,\omega)-\sum_{i=1}^{N}\psi_i(x)u_i^h(x,\omega))$$
$$=\sum_{i=1}^{N}(\nabla\psi_i(x)(u(x,\omega)-u_i^h(x,\omega))+\psi_i(x)\nabla(u(x,\omega)-u_i^h(x,\omega))). \quad (3.26)$$

Consequently, we get

$$\|u(x,\omega)-\sum_{i=1}^{N}\psi_i u_i^h(x,\omega)\|^2_{L^2(H_0^1(D),\Omega)}$$
$$=\int_\Omega\int_D|\nabla(u(x,\omega)-\sum_{i=1}^{N}\psi_i u_i^h(x,\omega))|^2\mathrm{d}x\mathrm{d}P \quad (3.27)$$
$$\le C\sum_{i=1}^{N}\int_\Omega\int_D(\nabla\psi_i(x)(u(x,\omega)-u_i^h(x,\omega))$$
$$+\psi_i(x)\nabla(u(x,\omega)-u_i^h(x,\omega)))^2\mathrm{d}x\mathrm{d}P, \quad (3.28)$$

where the constant C depends on the number of overlapping neighborhoods for each subdomain D_i.

Recall that we have assumed $\psi_i(x)\in[0,1]$, $\nabla\psi_i(x)\le\frac{C}{H}$, then we have

$$\|u(x)-\sum_{i=1}^{N}\psi_i u_i^h(x,\omega)\|^2_{L^2(H_0^1(D),\Omega)}$$
$$\le C\sum_{i=1}^{N}\int_\Omega\int_{D_i}\frac{1}{H^2}(u(x,\omega)-u_i^h\omega))^2+|\nabla(u(x,\omega)-u_i^h(x,\omega))|^2\mathrm{d}x\mathrm{d}P. \quad (3.29)$$

Finally, using the local error estimate (3.24) and the fact $N=O(1/h^d)$, we get

$$\|u(x,\omega)-\sum_{i=1}^{N}\psi_i u_i^h(x,\omega)\|^2_{L^2(H_0^1(D_i),\Omega)} \le \sum_{i=1}^{N}\epsilon^2H^d\|f(x)\|^2_{L^2(D)}$$
$$\le C\epsilon^2\|f(x)\|^2_{L^2(D)}. \quad (3.30)$$

Since $\sum_{i=1}^{N}\psi_i u_i^h(x,\omega)\in V_h$, we get that

$$\inf_{v(x,\omega)\in V_h}\|u(x,\omega)-v(x,\omega)\|_{L^2(H_0^1(D),\Omega)}\le C\epsilon\|f(x)\|_{L^2(D)}. \quad (3.31)$$

Based on the quasi-optimal property of the Galerkin projection (2.14), we get the following convergence result for the numerical solution $u_h(x,\omega)$. With high probability,

$$\|u(x,\omega) - u_h(x,\omega)\| \leq C\epsilon \|f(x)\|_{L^2(D)}. \tag{3.32}$$

□

4. Implementation of the Resulting Model Reduction Method

4.1. The implementation of the HKL expansion

To implement the HKL expansion, we need to first find a complete orthonormal basis in $H^1(D_i)$ and do the projection (3.9), where the $H^1(D_i)$ norm is defined as (3.16). We have assumed that the fine physical mesh of size h can resolve the spatial variation of the solution, so we will do the HKL expansion in the discrete setting. On each domain D_i, we construct the stiffness matrix S_i that corresponds to the norm (3.16). Then the columns of $S_i^{-1/2}$ form a complete set of orthonormal $H^1(D_i)$ basis functions for the discretized space of $H^1(D_i)$. For a discrete $H^1(D_i)$ function $u(x)$, $S_i^{1/2}u$ gives us the coefficient of the projection (3.9). After the $H^1(D_i)$ projection, we need to do KL expansion to $c(i,\omega)$ (3.10). We first compute its covariance $C(i,j)$ and then obtain the expansion following (3.6), (3.7), after which we finally get the HKL expansion of a $L^2(H^1(D_i),\Omega)$ function according to (3.11).

4.2. Selecting local stochastic basis functions from HKL expansion

In step 4 of the algorithm in section 3.4, where we described how to construct local stochastic basis, if the construction of local stochastic basis has not been completed on D_i, we add all the stochastic basis functions extracted from the HKL expansion of $u_e^i(x,\omega)$ to the set of local stochastic basis functions on D_i. However, those stochastic basis functions that correspond to very small singular values σ_i in the HKL expansion of $u_e^i(x,\omega)$ cannot capture the main stochastic structure of the solution space. So in our numerical implementation, we will only add those stochastic basis functions corresponding to singular values $\sigma_i > \alpha\sqrt{\pi/8}\epsilon H^{d/2}$ to the set of local stochastic basis. We also set a limit for the number of local stochastic basis

to be added at each time step. This makes sure that the constructed local stochastic basis can capture the main action of the solution operator in the stochastic direction.

4.3. Simplification of the trial space

Consider the trial space V_h that we construct in (3.21). One can see that the piecewise linear spatial basis $\phi_j(x)$ on the fine mesh of size h may arise multiple times, and this is because it may have support on multiple subdomains D_i. Let $j_1, j_2 ... j_p$ be the index of the subdomains D_i that ϕ_j has support on, then the following basis functions of the trial space (3.21) contain $\phi_j(x)$,

$$\phi_j(x)\psi_{j_1}(x) \otimes \{\xi_{j_1}^0(\omega), \dots \xi_{j_1}^{k_{j_1}}(\omega)\}, \dots \phi_j(x)\psi_{j_p}(x) \otimes \{\xi_{j_p}^0(\omega), \dots \xi_{j_p}^{k_{j_p}}(\omega)\}. \tag{4.1}$$

We choose $H >> h$ in our implementation, because of which we can make the assumption that

$$\phi_j(x)\psi_{j_p}(x) \approx \phi_j(x). \tag{4.2}$$

Then the representation of the finite dimensional space V_h can be simplified as the coupling of spatial basis $\phi_j(x)$ on the fine mesh with the local stochastic basis functions on $D_{j_1}, D_{j_2}, \dots D_{j_p}$.

$$V_h = \sum_{j=1}^{n} \text{span}\{\phi_j(x)\xi_{j_1}^0(\xi), \phi_j(x)\xi_{j_1}^1 \dots \phi_j(x)\xi_{j_p}^{k_{j_p}}\} \tag{4.3}$$

We re-label these local stochastic basis functions associated with $\phi_j(x)$ as $\xi_j^i(\omega), i = 0, \dots K_j$. Note that $\xi_j^i(\omega), i = 0, \dots K_j$ come from HKL expansions on different sub-domains D_i, thus can be linearly dependent. In this case the corresponding stiffness matrix formed in (3.30) will be singular. To overcome this, we apply an additional Gram-Schmidt orthogonalization procedure to $\xi_j^i(\omega), i = 0, \dots K_j$, during which we throw away the local stochastic basis functions that are redundant. We say $\xi_j^i(\omega)$ is redundant if $\inf_{c_k} \|\xi_j^i(\omega) - \sum_{k=0}^{i-1} c_k \xi_j^k(\omega)\|_{L^2(\omega)} \leq \epsilon/10$. We denote the resulting local stochastic basis

functions as $\xi_j^i(\omega), i = 0, \dots k_j$, then the trial space V_h is simplified to

$$V_h = \Big\{ \sum_{i=1}^{n} \sum_{j=0}^{k_i} c_i^j \phi_i(x) \xi_i^j(\omega) : c_i^j \in R \Big\}. \tag{4.4}$$

Note that in the above simplified trial space (4.4), the partition of unity functions (3.1) do not appear due to our simplification (4.2). However, the partition of unity formulation is necessary for our proof of the convergence of online numerical solutions (3.23).

4.4. Discretization in the spatial direction

In our numerical examples in this paper, we consider 2D problems on the square domain $D = [0, 1] \times [0, 1]$. We first discretize the domain D using uniform coarse square mesh of size $H = 1/I$, and get $N = (I - 1)^2$ interior coarse mesh nodes. We denote these interior node points as $x_i, i = 1, \dots (I - 1)^2$, then for each x_i, we choose the local square of size $2H$ and centered at x_i as the partition of unity subdomain D_i. We can easily construct partition of unity function $\psi_i(x)$ that has support on D_i and satisfies property (3.1).

Then we put a fine right triangular mesh of size h on D, which refines of the partition of unity constructed above. Correspondingly, we discretize the function space $H^1(D)$ using the span of piecewise linear functions on this fine mesh. This coarse-fine mesh discretization is illustrated in Figure 1.

After the simplification of the trial space V_h described in the previous subsection, for the spatial basis functions $\phi_j(x)$ that are supported on the same coarse-grid square of size $H \times H$, their associated local stochastic basis functions are the same.

4.5. Discretization in the stochastic direction

There are basically two ways of discretization in the stochastic direction. The first one is choosing a set of orthogonal polynomials, $H_1(\omega), \dots H_M(\omega)$, and representing the offline sampled numerical solutions and the constructed local stochastic basis functions as the linear combination of these orthogonal polynomials. If we use the Galerkin polynomial chaos method to solve the SPDE in the offline stage, then we are using this way of discretization. The

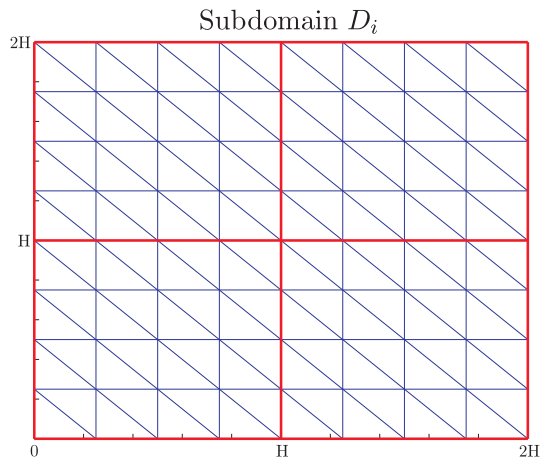

Figure 1: A sub-main D_i with fine mesh discretization. In the center is the coarse node point x_i.

local stochastic basis functions will be stored as length-M vectors, corresponding to the coefficients in their expansion using orthogonal polynomials $H_i(\omega), i = 1, \dots M$.

The second method, which is the one that we employ in our numerical examples, is to discretize the probability space and measure (Ω, P) using a set of sampling points and weights, $(\theta_i, w_i), i = 1, \dots M$. If we use stochastic collocation method in the offline stage, then θ_k correspond to the collocation points. θ_k and w_k are determined by the underlying distribution of ω. If we use Monte Carlo method in the offline stage, then θ_k are the selected sampling points, and $w_i = 1/M$. In our numerical examples in the next section, we use the stochastic collocation method in the offline stage, and the sampling points and corresponding weights are chosen based on the Smolyak sparse grid collocation points. [43, 37]

4.6. The online Galerkin projection

After we simplified the trial space according to section 4.3, we get a trial space taking the following form

$$V_h = \Big\{ \sum_{i=1}^{n} \sum_{j=0}^{k_i} c_i^j \phi_i(x) \xi_i^j(\omega) : c_i^j \in R \Big\}, \tag{4.5}$$

where $\xi_i^0(\omega) = 1$, and for each i, $\xi_i^j(\omega), j = 0, \dots k_i$ are orthonormal in $L^2(\Omega)$. Let $K = \sum_{i=1}^n k_i + n$, then the stiffness matrix M_S corresponding to (4.5) is of size $K \times K$. We define R as the relabelling function that maps each pair (i, j), $i = 1, \dots n$, $j = 0, \dots k_i$ to the global index of the basis $\phi_i(x)\xi_i^j(\omega)$: $R(i, j) = \sum_{l=1}^{i-1}(k_l+1)+j+1$. With this relabeling function, we can compute the stiffness matrix as

$$M_S(R(i_1, j_1), R(i_2, j_2)) = \int_\Omega \int_D \xi_{i_1}^{j_1}(\omega)\nabla\phi_{i_1}(x)a(x, \omega)\xi_{i_2}^{j_2}(\omega)\nabla\phi_{i_2}(x)\mathrm{d}x\mathrm{d}P. \tag{4.6}$$

Then we consider computing the load vector $b \in R^K$ corresponding to forcing function $f(x)$. We have

$$b(R(i, j), 1) = \int_\Omega \int_D \xi_i^j(\omega)\phi_i(x)f(x)\mathrm{d}x\mathrm{d}P. \tag{4.7}$$

Recall that the local stochastic basis functions $\xi_i^j(\omega), j \geq 1$ are orthogonal to $\xi_i^0(\omega) = 1$, i.e., they have mean 0. As a consequence, the corresponding entries in the load vector (4.7) vanish. Namely, only the entries $b(R(i, 0), 1), i = 1, \dots n$ are non-zero.

Then we solve equation

$$M_S c = b, \tag{4.8}$$

to get the coefficient c_i^j and recover the numerical solution via assembling the basis functions $\phi_i(x)\xi_i^j(\omega)$,

$$u_h(x, \omega) = \sum_{i=1}^{n} \sum_{j=0}^{k_i} c_i^j \phi_i(x)\xi_i^j(\omega). \tag{4.9}$$

If the quantities of interest are mean and variance of the solution, then they can be computed efficiently without assembling the basis functions. Namely,

$$\bar{u}(x_i) = c_i^0, \quad \sigma[u(x_i, \omega)] = (\sum_{j=1}^{k_i} (c_i^j)^2)^{1/2}. \tag{4.10}$$

4.7. Computational cost of the model reduction method

The model reduction method introduced in this work consists of two

stages, the offline stage and the online stage. The major computational cost in the offline stage includes the following.

1. Solving the SPDE (1.1) for several times using existing SPDE solver, like Galerkin polynomial chaos methods, or stochastic collocation methods using sparse grid. This corresponds to step 2 and step 4 of the algorithm in section 3.4 to construct local stochastic basis. We employ the stochastic collocation method in our numerical results in the next section.

2. To construct the local stochastic basis functions in step 4 of the algorithm in section 3.4, we need to do the HKL expansion to the residual $u_e^i(x,\omega)$. The major cost is computing the eigen-decomposition of the covariance matrix of $c(j,\omega)$. Fortunately, the HKL expansion is done on local regions of the domain D_i, which contains n_i fine mesh grid points. If n_i is small, then this part of cost is small. More importantly, the HKL expansions and the extractions of the local stochastic basis are independent on each sub-domain D_i, thus can easily be done in parallel.

3. In simplification of the representation of the trial space in section 4.3, we need a Gram-Schmidt orthogonalization procedure and throw away redundant stochastic basis. If the number of constructed local stochastic basis functions is small on each sub-domain D_i, then this computational cost is small. This can also be done in parallel for different sub-domains.

4. In formulating the stiffness matrix (4.6), we need to do a lot of integration in the stochastic direction. However, the integrations on different fine mesh triangle elements are independent from each other, thus they can be done in parallel to accelerate the calculation.

The online computational cost mainly comes from solving the linear system (4.8). M_S is a sparse matrix since $\phi_i(x)$ has compact support, and of size

$$(\sum_{i=1}^{n}(k_i+1)) \times (\sum_{i=1}^{n}(k_i+1)). \tag{4.11}$$

Recall that if we use the Galerkin polynomial chaos method to solve equation (1.1) and use M orthogonal basis functions, then it is equivalent to choosing the local stochastic basis

$$\xi_i^j(\omega) = H_j(\omega), \quad j = 1, \dots M, \tag{4.12}$$

in the HSFEM framework, and the corresponding linear system is of size

$$Mn \times Mn. \tag{4.13}$$

So if $\bar{k} = \frac{\sum_{i=1}^n k_i}{n}$ is less than M, then our method involves less degree of freedom. Based on our numerical results, the resulting $\bar{k}$ in our examples are significantly smaller than M.

5. Numerical Results

In this section, we apply the model reduction method developed in the previous sections to several problems to demonstrate its efficiency. We consider 2D problems that are defined on the domain $D = [0,1] \times [0,1]$ and take the following form:

$$\begin{cases} -\mathrm{div}(a(x,y,\omega)\nabla_{x,y} u(x,y,\omega)) = f(x,y), \\ u(x,y,\omega)|_D = 0. \end{cases} \tag{5.1}$$

In the spatial direction, we discretize the domain as shown in section 4.4, and choose $H = 1/8$, $h = 1/64$. We get 49 subdomains D_i and 3969 piecewise linear spatial basis functions $\phi_i(x)$. In the stochastic direction, we use the Smolyak sparse grid collocation points to discretize the problem, and denote the resulting collocation points and weights as $(\theta_k, w_k), k = 1, \dots M$. With the above discretization, we use stochastic collocation method in the offline stage to construct the local stochastic basis functions. In the *a posterior* error estimation procedure (3.14) in constructing local stochastic basis functions, we choose $r = 10$. Namely, we use 10 sampled solutions in step 2 of section 3.4 to verify the approximation property of the constructed local stochastic basis (3.3). In extracting local stochastic basis functions in step 4 of section 3.4, we base on the principles stated in section 4.2. We choose at

most 4 basis functions from the local HKL expansion of the residual $u_i^e(x,\omega)$ at each single step.

For the purpose of evaluating the effectiveness of our model reduction strategy, we assume that the spatial and stochastic discretization can resolve the variations of the solution. With this assumption, we neglect the error in the discretization of the problem, and use the stochastic collocation solution $u_{sc}(x,\omega)$ as the reference to measure the error in our online numerical solutions $u_h(x,\omega)$. Then the only source of error in $u_h(x,\omega)$ is from our model reduction, since we only select a very small number of local stochastic basis functions to approximate the solution space in the stochastic direction.

In each of our numerical examples, we compute the following quantities.

1. The average number of local stochastic basis functions associated with each spatial basis function. If $\bar{k} = \frac{\sum_{i=1}^{n} k_i}{n}$ is small, then the solution space to (1.1) is very compact in the stochastic direction on local regions of the spatial domain. Moreover, recall that in the online stage of our method, we use the Galerkin method to obtain the numerical solution, and we have in total
$$\sum_{i=1}^{n} k_i + n = n\bar{k} + n \tag{5.2}$$
degrees of freedom. So $\bar{k}$ measures the size of the constructed trial space and the efficiency of our model reduction method in the online stage.

2. The number of sampled solutions that we use to construct the local stochastic basis.

   Note that in step 4 of the algorithm in section 3.4, solutions to (1.1) using randomly chosen forcing functions are generated. The major computational cost in the offline stage comes from this step. If we can construct the local stochastic basis using a very small number of sampled solutions, then the offline computational cost will also be small.

3. The error in mean and standard deviation of the solution, which are the two primary quantities of interest in uncertainty quantification problems.
$$E[u_h(x,\omega)] - E[u_{sc}(x,\omega)], \tag{5.3}$$

$$\sigma[u_h(x,\omega)] - \sigma[u_{sc}(x,\omega)]. \tag{5.4}$$

4. The relative $L^2(D\times\Omega)$ error of the numerical solution,

$$E_k = \frac{\|u_h(x,\omega) - u(x,\omega)\|_{L^2(D\times\Omega)}}{\|u(x,\omega) - \bar{u}(x,\omega)\|_{L^2(D\times\Omega)}}. \tag{5.5}$$

Note that the denominator above is the L^2 norm of the stochastic part of the solution, so E_k measures the capacity of our method in capturing the stochastic part of the solution.

5.1. A 2D problem with Gaussian random input

The first example we consider is a 2D problem with Gaussian random input. The Gaussian random variables in the coefficient violate the uniform ellipticity condition (1.2) of the equation, thus our analysis in section 2 will not apply. However, our numerical results suggest that even in this case, our model reduction method still works well. The coefficient of the problem $a(x,y,\omega)$ is given by the following

$$\log a(x,y,\omega) = \frac{1}{4}\sum_{m=1}^{4} \omega_m(\sin(m\pi x) + \cos((5-m)\pi y)), \tag{5.6}$$

where $\omega_m, m = 1,\dots 4$ are independent standard Gaussian random variables.

In the stochastic direction, we discretize the problem using the 8-th order smolyak sparse grid collocation points, and get $M = 1305$ sampling points. In the *a posteriori* error estimation step in our construction of the local stochastic basis, namely, step 5 of section 3.4, we choose (3.18) to be

$$\alpha\sqrt{\pi/2}\epsilon H = 2\times 10^{-2}. \tag{5.7}$$

There are in total 6 sampled stochastic solutions generated in step 4 of section 3.4 to construct the local stochastic basis functions, which means that the offline computational cost of our model reduction method is small and only several times of that using traditional solvers. After the offline stage, the average number of local stochastic basis functions associated with each spatial basis function is

$$\bar{k} \approx 18. \tag{5.8}$$

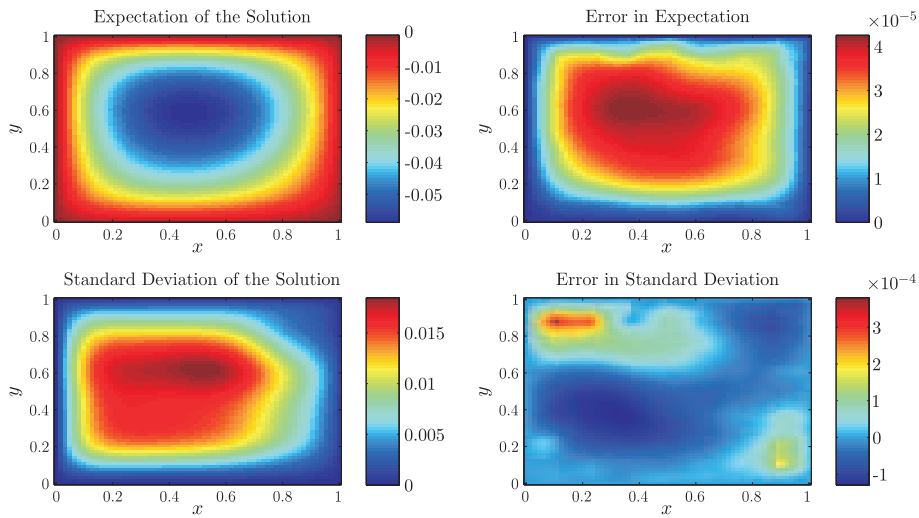

Figure 2: Error in expectation and standard deviation of our online numerical solution $u_h(x, \omega)$.

For this problem, the number of local stochastic basis functions is quite small compared with the degree of freedom in the stochastic direction for the stochastic collocation method, which is $M = 1305$. This means our method can achieve significant computational savings in the online stage.

In the online stage, we test our method using the following forcing function

$$f(x, y) = -1 + x - 2y. \tag{5.9}$$

Errors in mean and expectation of our numerical solution are plotted in Figure 2, from which we can see that our method achieves high accuracy in the two primary quantities of interest.

The relative error in the stochastic part of the solution, (5.5), is quite small,

$$E_k = 3.667 \times 10^{-2}. \tag{5.10}$$

And this implies that our model reduction method can capture the main part of the stochastic solution.

To sum up, by solving the equation (1.1) using existing solvers for only a few times in the offline stage, our model reduction method can effectively construct a small number of local stochastic basis functions that can accurately capture the stochastic structure of the solutions.

5.2. A 2D model problem with high-dimensional stochastic input

In this example, the random coefficient $a(x, y, \omega)$ in (5.1) is given by

$$\log a(x, y, \omega) = \frac{1}{4} \sum_{m=1}^{12} \omega_m (\sin(m\pi x) + \cos((13 - m)\pi y)), \tag{5.11}$$

where $\omega_m, m = 1, 2 \dots 12$ are independent random variables uniformly distributed on $[-1/2, -1/2]$.

Note that the $\omega_k, k = 1, \dots 12$ contribute equally to the $L^2(D \times \Omega)$ norm of $\log(a(x, \omega))$, thus none of them can be neglected, which means this problem has genuine high stochastic dimension. We use the 4th order sparse grid collocation points to discretize (Ω, P) as we did in the previous example, and get totally $M = 2096$ sampling points. In the *a posteriori* error estimation step in our construction of the local stochastic basis, namely, step 5 of section 3.4, we choose (3.18) to be

$$\alpha \sqrt{\pi/2} \epsilon H = 10^{-2}. \tag{5.12}$$

There are 9 sampled stochastic solutions generated in step 4 of section 3.4 to construct the local stochastic basis functions, which is not large. After the offline stage, the average number of local stochastic basis functions associated with each spatial basis function is

$$\bar{k} \approx 36. \tag{5.13}$$

For this problem with 12 dimension of stochastic input, the number of local stochastic basis functions is quite small compared with the degree of freedom in the stochastic direction for the stochastic collocation method, which is $M = 2096$. This means we can achieve significant computational savings in the online stage.

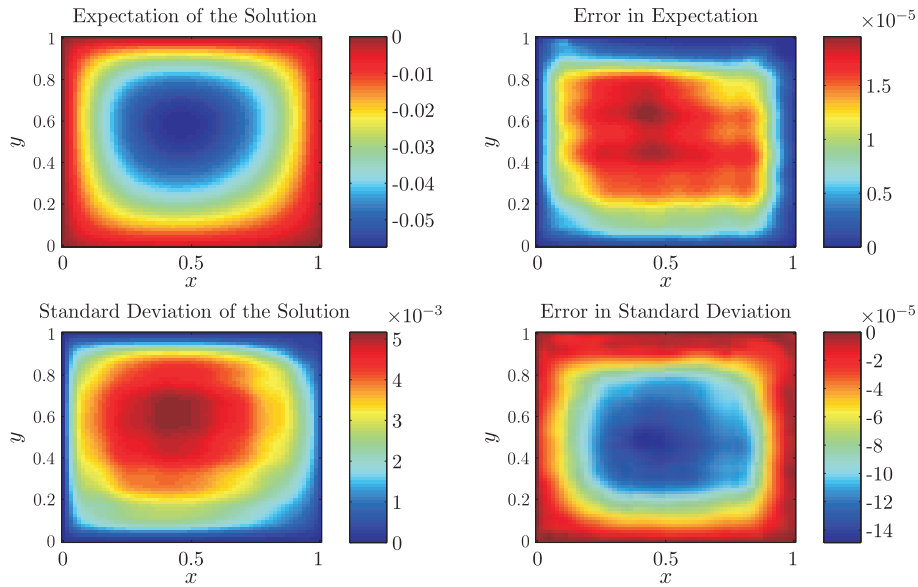

Figure 3: Error in expectation and standard deviation of our online numerical solution $u_h(x, \omega)$.

In the online stage, we test our method using the following forcing function

$$f(x, y) = -1 + x - 2y. \tag{5.14}$$

Errors in mean and expectation of our numerical solution are plotted in Figure 3, and from it we can see that our method achieves high accuracy in the two primary quantities of interest.

The relative error in the stochastic part of the solution, (5.5), is,

$$E_k = 6.697 \times 10^{-2}. \tag{5.15}$$

And this implies that our model reduction method can capture the main part of the stochastic solution.

For this example with high-dimensional stochastic input, we observe again that our model reduction method can construct effective local stochastic basis functions that capture the stochastic structure of the solution space to (1.1) on local regions of the physical domain. The offline computational cost is not too large, and our method can achieve significant computational saving in the online stage.

5.3. A 2D example with discontinuous coefficient

In this example, we consider the case in which the coefficient $a(x, y, \omega)$ has discontinuities. To introduce the random coefficient, we first divide the domain $D = [0, 1] \times [0, 1]$ into 4 parts:

$$\begin{aligned} D_1 &= [0, 1/2] \times [0, 1/2], \ D_2 = [1/2] \times [0, 1/2], \\ D_3 &= [0, 1/2] \times [1/2, 1], \ D_4 = [1/2, 1] \times [1/2, 1]. \end{aligned} \tag{5.16}$$

And the coefficient is given by

$$a(x, y, \omega) = \begin{cases} 1+\exp(\sum_{k=1}^{3} 2\omega_k(\sin(2k\pi x) + \cos(2(4-k)\pi y))), & (x, y) \in D_1, \\ 1+\exp(1+\sum_{k=4}^{6} 2\omega_k(\sin(2(k-3)\pi x)+\cos(2(7-k)\pi y))), & (x, y) \in D_2, \\ 1+\exp(2+\sum_{k=7}^{9} 2\omega_k(\sin(2(k-6)\pi x)+\cos(2(10-k)\pi y))), & (x, y) \in D_3, \\ 1+\exp(3+\sum_{k=10}^{12} 2\omega_k(\sin(2(k-9)\pi x)+\cos(2(13-k)\pi y)), & (x, y) \in D_4. \end{cases} \tag{5.17}$$

where $\omega_i, i = 1, \ldots 12$ are independent random variables uniformly distributed in $[-1/2, 1/2]$. Again, we can see that the 12 random variables $\omega_i, i = 1, \ldots 12$ contribute equally to the $L^2(D\times\Omega)$ norm of $\log(a(x, y, \omega)-1)$. Thus this problem has genuine high stochastic dimension.

Our discretizations in both the spatial and stochastic directions for this problem are the same as our previous example. We finally get $M = 2096$ collocation points. In the *a posteriori* error estimation step in our construction of the local stochastic basis, namely, step 5 of section 3.4, we choose (3.18) to be

$$\alpha\sqrt{\pi/2}\epsilon H = 4 \times 10^{-4}. \tag{5.18}$$

There are 18 sampled stochastic solutions generated in step 4 of section 3.4 to construct the local stochastic basis functions. After the offline stage, the average number of local stochastic basis functions associated with each spatial basis function is

$$\bar{k} \approx 31. \tag{5.19}$$

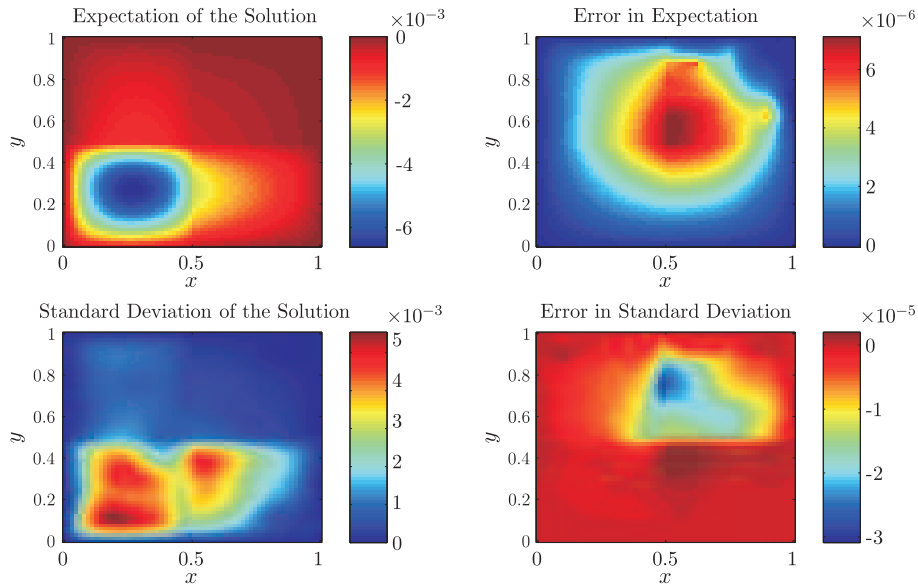

Figure 4: Error in expectation and standard deviation of our online numerical solution $u_h(x, \omega)$.

For this problem with 12 dimension of stochastic input, the number of local stochastic basis functions is quite small compared with the degree of freedom in the stochastic direction for the stochastic collocation method, which is $M = 2096$. This means we can achieve significant computational savings in the online stage.

In the online stage, we test our method using the following forcing function

$$f(x, y) = -1 + x - 2y. \tag{5.20}$$

Errors in mean and expectation of our numerical solution are plotted in Figure 3, and from it we can see that our method achieves high accuracy in the two primary quantities of interest.

The relative error in the stochastic part of the solution, (5.5), is quite small,

$$E_k = 6.717 \times 10^{-2}, \tag{5.21}$$

and this implies that our model reduction method can capture the main part of the stochastic solution.

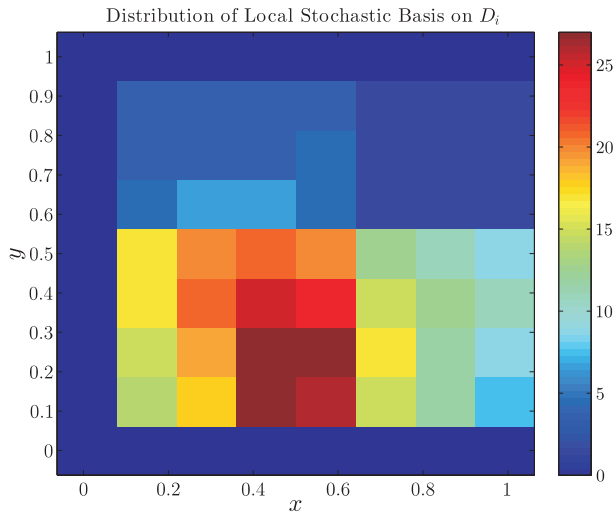

Figure 5: The distribution of local stochastic basis functions constructed on each sub-domain.

For each coarse grid node point x_i, there exists a subdomain D_i centered at x_i. The number of local stochastic basis functions generated on each D_i are different, the distribution of which is plotted in Figure 5. From this figure we can see that more local stochastic basis functions are constructed on region D_1, which according to (5.17), is the region where the random part of the coefficient has stronger effect. This result reveals that our model reduction method can recognize the heterogeneous stochastic structure of the solution space in the offline stage, and put more stochastic basis functions in regions where the solution has richer stochastic structure.

6. Concluding Remarks

A model reduction method for elliptic partial differential equations with random input is introduced. This method follows the Heterogeneous Stochastic FEM framework proposed recently, and employs the heterogeneous coupling of spatial basis with stochastic basis to approximate the solution space. This framework allows us to exploit the compactness of the solution space in the stochastic direction.

This method consists of two stages, the offline and online stages, and suits the multi-query setting. In the offline stage, we sample the stochastic

solutions using randomly chosen forcing functions for a number of times, and construct the local stochastic basis for the HSFEM framework through the local Hilbert-Karhunen-Loève expansions of the sampled solutions. The local stochastic basis functions are chosen adaptively, and can capture the stochastic structure of the solution space in local regions of the spatial domain. In the online stage, for different forcing functions, we obtain the numerical solutions using the trial space obtained in the offline stage through the Galerkin projection. We prove the convergence of the online numerical solutions based on the thresholding in the offline stage.

Several numerical examples are presented to demonstrate the implementation and efficiency of the method. Our numerical results suggest that the proposed method can effectively identify the compact structure of the solution space and construct reduced models without losing high accuracy.

Acknowledgments

We would like to thank the reviewers for their constructive comments which help improve the quality of this paper. This research was in part supported by Air Force MURI Grant FA9550-09-1-0613, DOE grant DE-FG02-06ER257, and NSF Grants No. DMS-1318377, DMS-1159138.

References

1. I. Babuška and P. Chatzipantelidis, On solving elliptic stochastic partial differential equations, *Computer Methods in Applied Mechanics and Engineering*, **191** (2003), No.37, 4093-4122.

2. I. Babuška, F. Nobile and R. Tempone, A stochastic collocation method for elliptic partial differential equations with random input data. *SIAM Review*, **52**(2010), No.2, 317-355.

3. I. Babuška, R. Tempone and G. E. Zouraris, Galerkin finite element approximations of stochastic elliptic partial differential equations, *SIAM J. Numer. Anal.*, **42**(2004), No.2, 800-825.

4. M. Barrault, Y. Maday, N. C. Nguyen and A. T. Patera, An empirical interpolationmethod: application to efficient reduced-basis discretization of partial differential equations, *Comptes Rendus Mathematique*, **339** (2004), No.9, 667-672.

5. J. Beck, R. Tempone, F. Nobile and L. Tamellini, On the optimal polynomial approximation of stochastic pdes by galerkin and collocation methods, *Mathematical Models and Methods in Applied Sciences*, **22** (2012), No.9, 1250023.

6. L. Berlyand and H. Owhadi, Flux norm approach to finite dimensional homogenization approximations with non-separated scales and high contrast, *Archive for Rational Mechanics and Analysis*, **198** (2010), No.2, 677-721.

7. M. Bieri, A sparse composite collocation finite element method for elliptic spdes, *SIAM J. Numer. Anal.*, **49** (2011), No.6, 2277-2301.

8. M. Bieri, R. Andreev and C. Schwab, Sparse tensor discretization of elliptic spdes, *SIAM Journal on Scientific Computing*, **31** (2009), No.6, 4281-4304.

9. M. Bieri and C. Schwab, Sparse high order FEM for elliptic sPDEs, *Computer Methods in Applied Mechanics and Engineering*, **198** (2009), No.13, 1149-1170.

10. R. E. Caflisch, Monte Carlo and quasi-monte Carlo methods, *Acta Numerica*, **7** (1998), 1-49.

11. R. H. Cameron and W. T. Martin, The orthogonal development of non-linear functionals in series of Fourier-Hermite functionals, *Ann. Math.*, (1947), 385-392.

12. M. Cheng, T. Y. Hou, M. Yan and Z. Zhang, A data-driven stochastic method for elliptic pdes with random coefficients, *Journal on Uncertainty Quantification*, **1** (2013).

13. M. Cheng, T. Y. Hou and Z. Zhang. A dynamically bi-orthogonal method for time-dependent stochastic partial differential equations I: Derivation and algorithms, *Journal of Computational Physics*, **242** (2013), 843-868.

14. M. Cheng, T. Y. Hou and Z. Zhang, A dynamically bi-orthogonal method for time-dependent stochastic partial differential equations II: Adaptivity and generalizations, *Journal of Computational Physics*, **242** (2013), 753-676.

15. M. Choi, T. P. Sapsis and G. E. Karniadakis, On the equivalence of dynamically orthogonal and bi-orthogonal methods: Theory and numerical simulations, *Journal of Computational Physics*, **270** (2014), 1-20.

16. A. Cohen, R. DeVore, and C. Schwab, Convergence rates of best N-term Galerkin approximations for a class of elliptic sPDEs, *Foundations of Computational Mathematics*, **10** (2010), No.6, 615-646.

17. A. Doostan, R. G. Ghanem, and J. Red-Horse, Stochastic model reduction for chaos representations, *Computer Methods in Applied Mechanics and Engineering*, **196** (2007), No.37, 3951-3966.

18. A. Doostan and H. Owhadi, A non-adapted sparse approximation of PDEs with stochastic inputs, *Journal of Computational Physics*, **230** (2011), No.8, 3015-3034.

19. M. Eigel, C. J. Gittelson, C. Schwab and E. Zander, A convergent adaptive stochastic Galerkin finite element method with quasi-optimal spatial meshes, *ESAIM: Mathematical Modelling and Numerical Analysis*, **49** (2015), No.5, 1367-1398.

20. R. G. Ghanem and P. D. Spanos, *Stochastic Finite Elements: A Spectral Approach*, volume 41, Springer, 1991.

21. D. Gilbarg and N. S. Trudinger, *Elliptic Partial Differential Equations of Second Order*, volume 224, springer, 2001.

22. L. Giraldi, D. Liu, H. G. Matthies and A. Nouy, To be or not to be intrusive? The solution of parametric and stochastic equations—Proper Generalized Decomposition, *SIAM Journal on Scientific Computing*, **37** (2015), A347-A368.

23. C. Gittelson, An adaptive stochastic galerkin method for random elliptic operators, *Mathematics of Computation*, **82** (2013), No.283, 1515-1541.

24. M. Grüter and K.-O. Widman, The green function for uniformly elliptic equations, *Manuscripta Mathematica*, **37** (1982), No.3, 303-342.

25. N. Halko, P.-G. Martinsson and J. A. Tropp, Finding structure with randomness: Probabilistic algorithms for constructing approximate matrix decompositions, *SIAM Review*, **53** (2011), No.2, 217-288.

26. T. Y. Hou and P. Liu. A heterogeneous stochastic FEM framework for elliptic PDEs, *Journal of Computational Physics*, **281** (2015), 942-969.

27. T. Y. Hou and P. Liu, Optimal local multi-scale basis functions for linear elliptic equations with rough coefficient. arXiv preprint arXiv:1508.00346, 2015.

28. M. Kleiber and T. D. Hien. *The Stochastic Finite Element Method: Basic Perturbation Technique and Computer Implementation*, Wiley New York, 1992.

29. L. Mathelin and K. A. Gallivan, A compressed sensing approach for partial differential equations with random input data, *Communications in Computational Physics*, **12** (2012), No.4, 919-954.

30. L. Li, H. A. Tchelepi and D. Zhang, Perturbation-based moment equation approach for flow in heterogeneous porous media: applicability range and analysis of high-order terms, *Journal of Computational Physics*, **188**, No.1, 296-317.

31. E. Liberty, F. Woolfe, P.-G. Martinsson, V. Rokhlin and M. Tygert, Randomized algorithms for the low-rank approximation of matrices, *Proceedings of the National Academy of Sciences*, **104** (2007), No.51, 20167-20172.

32. L. Mathelin, M. Y. Hussaini and T. A. Zang, Stochastic approaches to uncertainty quantification in cfd simulations, *Numerical Algorithms*, **38** (2005), No.1-3, 209-236.

33. J. M. Melenk, On n-widths for elliptic problems, *Journal of Mathematical Analysis And Applications*, **247** (2000), No.1, 272-289.

34. J. M. Melenk and I. Babuška, The partition of unity finite element method: basic theory and applications, *Computer Methods in Applied Mechanics and Engineering*, **139** (1996), No.1, 289-314.

35. E. Musharbash, F. Nobile, and T. Zhou, On the dynamically orthogonal approximation of time dependent random PDEs, Technical report, 2014.

36. H. Niederreiter, *Random number generation and quasi-Monte Carlo methods*, volume 63, SIAM, 1992.

37. F. Nobile, R. Tempone, and C. G. Webster, A sparse grid stochastic collocation method for partial differential equations with random input data, *SIAM Journal on Numerical Analysis*, **46** (2008), No.5, 2309-2345.

38. A. Nouy, A priori model reduction through proper generalized decomposition for solving timedependent partial differential equations, *Computer Methods in Applied Mechanics and Engineering*, **199** (2010), No.23, 1603-1626.

39. A. T. Patera and G. Rozza, Reduced basis approximation and a posteriori error estimation for parametrized partial differential equations, 2007.

40. G. Rozza, D. B. P. Huynh and A. T. Patera, Reduced basis approximation and a posteriori error estimation for affinely parametrized elliptic coercive partial differential equations, *Archives of Computational Methods in Engineering*, **15** (2008), No.3, 229-275.

41. T. P. Sapsis and P. F. J. Lermusiaux, Dynamically orthogonal field equations for continuous stochastic dynamical systems, *Physica D: Nonlinear Phenomena*, **238** (2009), No.23, 2347-2360.

42. K. Sargsyan, C. Safta, H. N. Najm, B. J. Debusschere, D. Ricciuto and P. Thornton, Dimensionality reduction for complex models via bayesian compressive sensing, *International Journal for Uncertainty Quantification*, **4** (2014), No.1.

43. S. A. Smolyak, Quadrature and interpolation formulas for tensor products of certain classes of functions, *Dokl. Akad. Nauk SSSR*, **4** (1963), 123.

44. O. Steinbach, *Numerical Approximation Methods for Elliptic Boundary Value Problems: Finite and Boundary Elements*, volume 99. Springer, 2008.

45. L. Tamellini, O. L. Maitre and A. Nouy, Model reduction based on proper generalized decomposition for the stochastic steady incompressible navierVstokes equations, *SIAM Journal on Scientific Computing*, **36** (2014), No.3, A1089-A1117.

46. J. L. Taylor, S. Kim and R. M. Brown, The green function for elliptic systems in two dimensions, *Communications in Partial Differential Equations*, **38** (2013), No.9, 1574-1600.

47. S. Watanabe, Karhunen-Loeve expansion and factor analysis, theoretical remarks and applications, In *Proc. 4th Prague Conf. Inform. Theory*, 1965.

48. N. Wiener, The homogeneous chaos, *Amer. J. Math.*, **60** (1938), No.4, 897-936.

49. D. Xiu and J. S. Hesthaven, High-order collocation methods for differential equations with random inputs, *SIAM Journal on Scientific Computing*, **27** (2005), No.3, 1118-1139.